Research Square

Preprints are preliminary reports that have not undergone peer review.
They should not be considered conclusive, used to inform clinical practice,
or referenced by the media as validated information.

Lignin Phenol Formaldehyde Resins Synthesised Using South African Spent Pulping Liquor

Chelaine Maree
Stellenbosch University
Johann F. Görgens
Stellenbosch University https://orcid.org/0000-0002-9961-754X
Luvuyo Tyhoda (ltyhoda@sun.ac.za)
Stellenbosch University https://orcid.org/0000-0003-4514-2283

Research Article

Keywords: soda lignin, lignosulphonate, bio-adhesive, lignin phenol formaldehyde, phenolation

Posted Date: November 30th, 2021

DOI: https://doi.org/10.21203/rs.3.rs-1026498/v1

License: This work is licensed under a Creative Commons Attribution 4.0 International License.
Read Full License

Version of Record: A version of this preprint was published at Waste and Biomass Valorization on March 22nd, 2022. See the published version at https://doi.org/10.1007/s12649-022-01756-3.

Abstract

Purpose The current study investigated to which extent phenol could be replaced by lignins to produce lignin phenol formaldehyde (LPF) resins, utilising soda lignin and sodium lignosulphonate as by-products from the South African pulping industry.

Method The lignins were characterised and soda lignin indicated the highest reactivity. It was therefore utilised to produce LPF resins at 60%, 80%, and 100% phenol substitution, using central composite designs to maximise the adhesive strength. A one-pot method allowing direct transition from phenolation to resin synthesis was used for the first time with a pulping lignin at 60% and 80% substitution.

Results Plywood made with LPF60, LPF80, and LPF100 resins attained their highest shear strengths of 0.786, 1.09, and 0.987 MPa, respectively, which adhered to the GB/T 14732-2013 standard (≥ 0.7 MPa). A substitution level of 68% produced the highest shear strength of 1.11 MPa. High-density particleboard made with this LPF68 resin gave a MOR and MOE of 40 and 3209 MPa, respectively, adhering to the ANSI A208.1 requirements. Thickness swelling and water absorption was 13.5% and 37.2%, respectively.

Conclusion The soda-lignin isolated by precipitation from sugarcane bagasse pulping liquor is the first industrial lignin shown to produce LPF100 resins adhering to standard requirements, without modification or additives.

Statement Of Novelty

Previous reports have proven that lignin is a viable substitute for phenol to produce lignin phenol formaldehyde resins. However, either with modification to improve the lignin reactivity, or at low lignin substitution levels, or with additives added during adhesive formulation. The present study demonstrated that the acid precipitated and acid purified soda lignin from sugarcane bagasse pulping liquor is the first industrial lignin shown to work as 100% substitute for phenol in the resin synthesis, to produce a resin adhering to industrial standard requirements, without requiring any lignin modification or resin additives. Furthermore, a one-pot phenolation and resin synthesis at substitution levels below 100% proved to increase the reactivity of the lignin-phenol before resin synthesis.

Introduction

Phenol formaldehyde (PF) resins are widely used in exterior wood applications, such as plywood, particleboard, etc. [1], due to their high bonding strength and resistance to water, temperature, and weathering [2]. They are synthesised from petroleum-derived chemicals in the presence of alkaline catalysts. However, due to the price fluctuations, high cost of crude oil and environmental concerns, there is a need to find bio-based phenol-replacements for these phenol-derived products [3].

Lignin is abundant in plant biomass and is available as a by-product from pulping industries, with over fifty million tons of lignin generated from the pulp and paper industry annually [4]. However, it is mostly

combusted for energy and has rarely been used for high-value applications. Lignin has a phenolic structure and has been investigated as a phenol substitute to synthesise lignin phenol formaldehyde (LPF) resins [5], as it is also renewable, less toxic and less expensive than conventional, fossil-based sources of phenol [6]. Therefore, substituting phenol with lignin could contribute to waste valorisation in the pulping industry and lead to environmental and economic benefits.

However, the side chains attached to the phenolic rings in lignins present challenges, as it causes lignin to have a lower reactivity during resin synthesis than phenol itself, as it has fewer reactive sites, less free hydroxyl groups and higher steric hindrance [7]. Therefore, several modification methods have been investigated to increase the reactivity of lignin, with the three major methods for LPF resin applications being demethylation, methylolation and phenolation [8]. Phenolation is currently the most promising method for LPF applications as it increases the reactivity by introducing more reactive sites and phenolic hydroxyl groups, while also cleaving weak bonds [9–12]. During phenolation, condensation of phenol and lignin occurs, which increases the available reactive sites and also cleaves weak ether bonds [13]. Phenolation is generally performed with acid catalysts [11, 14, 15] but has also been performed in alkaline conditions [10, 16, 17]. Using alkaline catalysts is favourable as it allows a direct transition from the phenolation reaction to the synthesis reaction, which could result in less chemical waste and reduced costs. Furthermore, a one-pot gradual polymerisation method with sodium hydroxide as a catalyst is possible, where the direct transition from phenolation to LPF synthesis is possible. The lignin was reacted with phenol to produce a lignin-phenol solution, whereafter formaldehyde was slowly added to start the synthesis reaction [9].

Several studies have investigated the substitution of phenol by lignin at substitution levels below 100% [10, 15, 18–21]. Recently, studies [22–25] have succeeded to replace phenol to produce lignin formaldehyde (LF) resins at a 100% substitution. However, additives were required during the adhesive formulation to be able to achieve acceptable properties for plywood applications. Therefore, this study aimed to produce LPF resins at a 100% substitution without requiring modification of the lignin or additives during hot-pressing. Two lignins from the South African pulping industry were investigated, soda lignin from sugarcane bagasse and lignosulphonate from *Eucalyptus grandis*, which were characterised to identify which would be the most promising substitute for phenol in LPF resin applications.

Materials And Methods

2.1 Materials

The two different lignins investigated were a sugarcane bagasse lignin from Sappi Ltd Stanger mill, South Africa, isolated from the spent pulping liquor of a soda pulping process, and a sodium lignosulphonate from pulping of *Eucalyptus grandis* (hardwood) obtained from Sappi Ltd Tugela mill, South Africa, which uses a Neutral Sulphite Semi-Chemical (NSSC) pulping process with sodium sulphite. Rotary cut pine (*Pinus elliottii*) veneer sheets and pine particles were supplied by York Timber,

Mpumalanga, South Africa. A sample of Bondtite 345 resin, used as a control in resin testing, was supplied by Bondtite Pty Ltd., South Africa. Snakeskin dialysis tubing (3500 Da, 35 mm diameter, 10.5 m) was supplied by Thermo Fischer Scientific. The chemicals used in this study were all reagent grade and included the following: Phenol crystals (98%), Folin-Ciocalteu (F-C) phenol reagent, sodium hydroxide pellets, xylose (≥ 99%), and vanillin (99%), and were supplied by Sigma Aldrich. Reagent grade sulphuric acid (≥ 98%) and formaldehyde (35%) were supplied by Science World Company SA. Sodium carbonate was supplied by Associated Chemical Enterprises Pty Ltd.

2.2 Methods

2.2.1 Lignin isolation and purification methods

These lignins were characterised before and after purification and labelled in the format (Lignin type) – (Isolation process) – (Purification process) as shown in Table 1. The lignin type was denoted ‘S’ for soda lignin and ‘L’ for lignosulphonate. The isolation process was denoted ‘A’ for acid precipitation and ‘S’ for spray-drying. The purification process was denoted ‘P’ for acid precipitation and ‘D’ for dialysis. Phenolation modification was denoted ‘P’.

Table 1 Sample IDs for different lignin samples that were used

Lignin type	Isolation process	Purification process	Modification	ID
Soda lignin	**A**cid precipitated			S-A
Soda lignin	**A**cid precipitation	**A**cid purification		S-A-P
Phenolated **S**oda lignin	**A**cid precipitation	**A**cid purification	**P**henolation	P-S-A-P
Lignosulphonate	**S**pray-dried			L-S
Lignosulphonate	**S**pray-dried	**D**ialysis		L-S-D

The soda lignin was received as black liquor and it was isolated through acid precipitation with 98% sulphuric acid, following a method described by García et al. [26]. Sulphuric acid was added dropwise to the black liquor while stirring until a pH value of 2 was reached, from an initial pH value of around 12.5. The solution was then left for 24 hours, whereafter the lignin was recovered by centrifugation at 7000 rpm for 10 minutes. The lignin was then washed twice with distilled water and dried overnight in a fume hood. The lignin was then milled to a particle size below 425 µm. This lignin powder was then placed in airtight plastic bags and labelled as S-A lignin until further use. The precipitated soda lignin powder was further purified by suspending it in a 1 N sulphuric acid solution, with a ratio of 200 ml acid solution per gram of dried lignin [26]. The solution was left to stand for 24 hours and then filtered to separate the lignin solids. The lignin was then washed three times with distilled water. The purified lignins were then

air-dried for 24 hours in a fume hood, then placed in airtight plastic bags and labelled as S-A-P until further use. The yield of the acid purification process was around 70%.

Sodium lignosulphonate was received as a spray-dried powder (labelled L-S). Previous studies [24] using the same lignosulphonate source have shown that the material had a high content of impurities. It was therefore purified using a dialysis membrane aiming to remove the hemicelluloses, simple sugars, and inorganic contaminants present. Dialysis was performed following the instructions from the supplier. The sodium lignosulphonate powder was dissolved in distilled water to make a 25 wt% solution. The solution was then poured into the dialysis tubing (3500 Da, 35 mm diameter), which was placed in a plastic bucket with distilled water with a buffer to solution volume ratio of 20. Three buffer exchanges were performed: after four hours, after another four hours, and then it was left for another twelve hours. The solution was then poured into tinfoil trays and dried for 24 hours in a 40 °C oven and then labelled as L-S-D and stored.

2.2.2 Lignin characterisation

The moisture and ash contents of the lignins were determined using methods based on the National Renewable Energy Laboratory (NREL) standards: NREL/TP-510-42621 (NREL 2008) and NREL/TP-510-42622 (NREL 2005), respectively. The elemental analyses of the lignins using a Vario EL Cube Elemental Analyser to determine the carbon (C), hydrogen (H), nitrogen (N), and sulphur (S) compositions.

The phenolic hydroxyl group content of the lignins and the dried lignin-phenol solutions were determined using an F-C reagent, following a method described by Areskogh [27]. The phenolic hydroxyl group content of the phenol (98%) was measured to be 9.91 mmol/g, which corresponded with previous reports [9]. Soda lignin-based samples were dissolved in NaOH solution, while lignosulphonate-based samples were dissolved in distilled water. A blank sample was also prepared as a reference for the NaOH and distilled water based solutions. All samples were done in triplicate. The absorbances were measured at 760 nm using a UV spectrophotometer (CECIL 2021 AQUARIUS 2000 series, 190 to 1000 nm). A calibration curve was set up using vanillin as a standard.

Mid-infrared (mid-IR) spectroscopy analysis was performed on the lignin in powdered form, operated in Attenuated Total Reflectance (ATR) mode at a resolution of 4 cm^{-1}, with 32 scans per sample within the band region of 4000 to 400 cm^{-1} [24]. The powder was pressed against the diamond crystal surface, using a Bruker Alpha P ATR-IR instrument. A background measurement was performed before each spectrum was recorded. Wiley Knowitall Spectroscopy Edition 2020 software was used to plot the spectra and the absorption bands were allocated using previous reports. The spectral data were baseline-corrected and normalised to one so that the spectra could be compared with each other.

A thermogravimetric analysis (TGA) was done using a TGA Q50 apparatus to determine the thermal behaviour of the different lignin samples. Approximately 5 ± 0.5 mg of sample was loaded onto an aluminium crucible which was placed in a TGA pan. A heating rate of 10 °C/min was used to heat the

sample from around 20 °C up to 595 °C under argon atmosphere at 70 ml/min [24]. TRIOS software was used to plot the TGA and derivative thermogravimetric (DTG) curves.

2.2.3 One-pot phenolation and LPF resin synthesis

A one-pot phenolation and resin synthesis method as reported by Zhao et al. [9] was used, where industrial steam explosion wheat straw lignin was used at 10% to 70% substitution. The reaction setup consisted of a five-neck round bottom flask which was placed in a heating mantle and equipped with a laboratory-scale overhead digital stirrer, dropping funnel, thermometer, flange lid, and a reflux condenser, as shown in Figure 1. The phenolation reaction was performed by weighing the required amount of phenol and lignin into the flask. Two-thirds of the required amount of the 1 M NaOH solution (as done by Kalami et al. [23]) was then added to the flask and it was mixed until all the phenol and lignin had dissolved. The temperature was slowly increased to the phenolation temperature (between 80 to 110 °C), whereafter the phenolation reaction was left to occur for 1.5 hours, with continuous stirring. The phenolation reaction was then left to cool to a temperature below 40 °C, whereafter the required amount of formaldehyde was added dropwise using a dropping funnel, whilst stirring continuously, to start the addition reaction. Once all the formaldehyde was added, the temperature was slowly increased to 65 °C and allowed to react for ten minutes for the addition reaction to occur. Thereafter, the condensation reaction was then initiated. The last third of 1 M NaOH was added via the dropping funnel, while the temperature was slowly increased to 85 °C. Once the temperature was reached, the reaction was allowed to continue for one hour. The mixture was left to cool to room temperature. The obtained resin was stored in the freezer at -8 °C. The resins were later poured into tinfoil trays and placed in a vacuum oven for drying at a temperature of 45 °C and continuously purged with nitrogen gas. The dried resins were then milled using an Ultra Centrifugal Mill ZM 200 (Retsch) into powders with a particle size below 0.5 mm and stored in airtight plastic bags.

2.3 Experimental design

2.3.1 Screening experiments

Screening experiments were conducted with the S-A-P, L-S, and L-S-D lignins to see which lignins would be viable to produce LPF resins, aiming for total substitution of phenol by lignin while adhering to the plywood manufacturing standards. The unmodified 100% substituted LPF resins were synthesised with a sodium hydroxide to phenolated lignin (NaOH/PL) molar ratio of 0.36, and a formaldehyde to phenolated lignin (F/PL) molar ratio of 2.

Face-centred central composite design

LPF resins were prepared by substituting either 60%, 80% or 100% of phenol with S-A-P lignin (weight percentage lignin, with the residual percentage phenol). A face-centred central composite design (CCD) was used to optimise the shear strength at each substitution level by varying three parameters that have a significant effect on the shear strength [18, 28, 29]. At 60% and 80% substitution, phenolation was performed, and the phenolation temperature, NaOH/PL ratio, and F/PL ratio were varied as shown in Table 2. At 100% substitution, no phenolation modification was done as no phenol was incorporated; therefore, only the NaOH/PL ratio and F/PL ratio was varied, as shown in Table 3. The amount of reacting substances of each run was scaled (keeping the ratios specified by the CCD) so that it would yield approximately 200 ml of each resin so that it would fit in the experimental setup and produce enough resin for further characterisation. Four centre point repeats were done for each CCD, which were representative of the standard deviation of the shear strength results of that CCD. The levels of the parameters tested are shown in Table 4.

The different LPF resins were labelled (as shown below) where the number directly after 'LPF' indicated the substitution percentage, followed by brackets which indicated the level of each parameter used in the order: NaOH/PL molar ratio, F/PL molar ratio, and then the phenolation temperature. In the case of LPF100 resins which only had the first two parameters optimised in its CCD, the third was omitted.

LPF *[substitution %]*_(*[NaOH/PL], [F/PL], [Temperature]*)

Table 2 The three-factor, three-level CCD used to maximise the shear strength of the LPF60 and LPF80 resins

Run number	NaOH/PL molar ratio	F/PL molar ratio	Temperature (°C)
1	-1	-1	-1
2	-1	1	-1
3	-1	1	1
4	-1	-1	1
5	1	-1	-1
6	1	1	-1
7	1	1	1
8	1	-1	1
9	-1	0	0
10	0	1	0
11	1	0	0
12	0	-1	0
13	0	0	-1
14	0	0	1
15	0	0	0
16	0	0	0
17	0	0	0
18	0	0	0

Table 3 The two-factor, three-level CCD used to maximise the shear strength of the LPF100 resins

Run number	NaOH/PL molar ratio	F/PL molar ratio
1	-1	-1
2	-1	1
3	1	-1
4	1	1
5	-1	0
6	1	0
7	0	0
8	0	-1
9	0	1
10	0	0
11	0	0
12	0	0
13	0	0

Table 4 The phenolation temperatures, NaOH/PL ratios, and F/PL ratios used in the CCD to maximise the shear strength at each substitution level

CCD level	-1	0	1
NaOH/PL molar ratio	0.12	0.36	0.63
F/PL molar ratio	1	2	3
Temperature (°C)	80	95	110

2.3.3 Statistical analysis

The analysis of variance (ANOVA) and regression equations were determined from the CCDs using Statistica software version 13.5.0.17. The null hypothesis predicted that all the regression coefficients are equal to zero. If $p < \alpha$, and $F > F_{critical}$, the null hypothesis could be rejected, and the parameters were proven to be statistically significant

2.3.4 Resin characterisation

Selected LPF resins were characterised similarly to the lignins with the methods described in section 2.2.2, for mid-IR spectroscopy analysis and TGA. The LPF resins analysed at each substitution level

included the centre point samples, as well as two good and two weak performing samples. The spectra were further compared in a principal component analysis (PCA) which was performed using Statistica software version 13.5.0.17.

The free formaldehyde contents of the best performing and centre point LPF resins at each substitution level were determined according to the European Standard DIN EN ISO 9397 [22]. Potentiometric titration was performed to quantify the amount of HCL released during the reaction of hydroxylamine hydrochloride (NH_2OH HCL) with formaldehyde (CH_2O) to form formaldoxime (CH_2 = NOH), releasing H_2O and HCl. One hundred millilitres of distilled water were added to approximately two grams of resin, and the pH of the solution was adjusted to a value of 4, using a 0.1 N hydrochloric acid solution. Twenty millilitres of a ten percent hydroxylamine hydrochloride solution were then added to the resins, whereafter the solution was titrated using a 0.1 N sodium hydroxide solution to a pH value of 4 again.

2.3.5 Plywood preparation and shear strength testing

Plywood boards were made and bonding strengths were tested according to the ASTM D 906-98 (2017) standard for shear strength of plywood samples by tension loading. Rotary cut pine veneers were used to make three-layered plywood boards with a thickness around 6 mm after pressing. The plywood was conditioned at 22 °C and 60% relative humidity for seven days [30]. The veneers were cut into 100 mm x 60 mm boards, with a thickness varying between 1 to 3 mm. The adhesive formulation was done by mixing the LPF resins with distilled water. The ratio of the lignosulphonate resin to water used was 60:40, while the soda lignin resin to water ratio used was 45:55. The adhesive was then applied with a spread rate of 400 g/m^2 on the surfaces of the two outer veneers and left for ten minutes to evaporate the excessive moisture. Each board was then hot-pressed individually for ten minutes at 160 °C and 1.6 MPa. The boards were left to cure in a conditioning room for seven days at 22 °C and 60% relative humidity before shear strength testing was performed. Each plywood board was cut into an 82.6 mm by 25.4 mm as specified. The boards were tested in an MTS Criterion Model 43 testing machine. The crosshead speed was set to 7 mm/min to obtain a loading rate between 4535 and 7560 g/s. The shear strength could then be calculated by dividing the maximum load obtained, by the surface area.

Strength and sorption properties of the resin as evaluated in particleboard manufacture

Particleboard was produced with the LPF68 resin to evaluate the performance of the resin with respect to strength and moisture resistance. Another board was produced with Bondtite, a commercial resin as a reference. Pine particles were milled and sieved to a size smaller than one millimetre and conditioned at 22 °C and 60% relative humidity for 96 hours. The equilibrium moisture content of the particles was determined to be 10%. The resin and Pine particles were mixed manually and poured into a steel mould (300 x 300 mm), with a 27 mm thick steel plate placed on top to compress the composite in the mould. The boards were pressed at 165 °C and 20 MPa for 10 minutes [30]. The boards were then removed from

the mould and conditioned at 22 °C and 60% relative humidity for 96 hours before testing. The amount of resin used was 10%, whereof the solid content of the resin was 48%.

The properties of the particleboards were then tested as specified in the ASTM D1037- 12 standard to quantify the modulus of rupture (MOR), modulus of elasticity (MOE), thickness swelling (TS), and water absorption (WA). The particleboards were tested using an Instron testing machine equipped with a 5 kN load cell. The boards were cut using a vertical bandsaw into 195 x 51 mm boards, and tests were performed with four replicates for each resin. A load was applied to the boards at a loading rate of 3 mm/min, while the load and deflection were recorded for each sample with an accuracy of ± 0.5% of the reading. After mechanical testing, the boards were cut again into dimensions of 85 x 51 mm for dimensional stability, using six replicates for each resin to determine the WA and TS of the boards.

Results And Discussion

3.1 Characterisation of the lignin samples

The soda lignin (before and after acid purification) and sodium lignosulphonate (before and after dialysis) were both characterised for their moisture and ash contents, elemental composition, and amount of phenolic hydroxyl groups, as shown in Table 5. Minimal impurities (such as inorganics, carbohydrates, etc.) are desired, as these could be cross-linked onto the lignin polymer occupying possible reactive sites, thereby reducing the reactivity [31]. Of the lignins investigated, S-A-P had the lowest ash content, which foreshadowed a higher reactivity with formaldehyde. The ash content of S-A was 14.9% and was reduced after acid purification to 2.16% in S-A-P. Dialysis only reduced the ash content from 24.8% in L-S to 12.8% in L-S-D. Furthermore, the sulphur content of 7.5% in L-S decreased only slightly after dialysis to 5.6% in L-S-D, which indicated that some of the impurities were attached to the lignin structure or remained due to a large molecular weight thereof [32]. Sulphur could be attached to the lignin structure as sulphonic acids or as sulphide bonds, cross-linking the lignosulphonate monomers [32]. The sulphur content of 2.60% in S-A was from the remaining sulphuric acid from the isolation process, as soda pulping is a sulphur-free process. This sulphur was removed during acid purification, as no sulphur was detected in S-A-P.

Table 5 Moisture content, ash content, elemental composition, and phenolic hydroxyl contents of the different lignins

	Moisture content (%)	Ash content (%)	C (%)	H (%)	N (%)	S (%)	Phenolic OH (mmol/g sample)
S-A	9.63	14.9	49.4	6.5	0.30	2.60	1.05
S-A-P	13.8	2.16	53.4	7.1	0.28	BDL[a]	1.70
L-S	4.01	24.8	35.4	4.7	0.19	7.5	1.53
L-S-D	10.4	12.8	41.7	6.0	0.26	5.6	1.48

[a] BDL – below detection limit

The phenolic hydroxyl content of S-A was 2.91% after acid precipitation and increased to 3.56% in S-A-P after further acid purification, apparently due to depolymerisation by cleavage of α- and β-O-4 bonds during acid purification [33]. This higher phenolic hydroxyl group content is desirable as these are very reactive functional groups, which can form quinone intermediates that activate the free ring positions to make the lignin reactive with formaldehyde in the LPF synthesis reaction [18, 34]. The phenolic hydroxyl groups of S-A-P and L-S were similar to previous reports that used the same quantification method [22, 35–37].

The mid-IR spectra of the lignin samples, as shown in Figure 2, were in accordance with that reported previously [18, 38–42], with the main band assignments in Table 6. The bands indicating G-monomers at 1374 cm^{-1} and 1220-1213 cm^{-1}, were present in S-A-P and L-S, while L-S-D showed a reduced absorbance. Furthermore, the absence of the band in L-S-D at 832 cm^{-1} attributed to the C-H stretching of H-monomers [42], indicated that some of the lower molecular weight monomers were removed during dialysis. The band at 895 cm^{-1} resulted from β-glycosidic bonds between monosaccharides and indicates that at least oligosaccharides were present, where the absence of this peak in L-S-D indicated that some of these sugars were removed during dialysis [41].

Table 6 Band assignments of the mid-IR spectra

Band (cm^{-1})	Assignment	Reference
3380-3324	O-H stretching vibration of phenolic OH and aliphatic OH	[38]
2933-2920	C-H stretching vibration in CH_2 and CH_3	[38]
2855-2845	C-H stretching vibration in OCH_3	[38]
~1600	C-H stretching vibration in aromatic skeleton	[38]
1523-1520	Aromatic ring vibrations	[40]
1460-1456	C-H deformation in asymmetric -CH_2 and -CH_3	[38]
1430-1418	C-C stretching vibration in aromatic skeleton	[38]
1374	C=O stretching of G-monomers	[33, 43]
1330-1327	In-plane deformation vibrations of phenolic OH in G- and S-monomers	[38]
1220-1213	C-O stretching of phenolic C-OH and phenolic C-O (Ar) in G- monomers	[33]
1159 - 1112	In-plane deformation vibrations of C-H (Ar)	[38]
1042-1032	C-O(H) and C-O(C) stretching vibration in first-order aliphatic OH and ether	[38]
898	β-glycosidic bonds between monosaccharides	[41]
834-831	Out-of-plane deformation vibrations of C-H (Ar) in H-monomers	[42]
750	Tri-substituted benzene ring structure	[18]
692	Mono-substituted benzene ring structure	[9]

Since LPF resins are cured around 165 °C, lignins with high thermal stability would be preferred to avoid their degradation during the curing reaction. Figure 3 shows the TGA and its first derivative (DTG) curves of the lignin samples. S-A-P had the highest thermal stability, with its maximum thermal degradation at 425 °C, which could be attributed to the high content of G-monomers as discussed from the mid-IR spectra in Figure 2, which have condensed C-C bonds that are more thermally stable [33]. This was followed with maximum thermal degradations of S-A at 375 °C, then L-S at 283 °C. The significant inorganic matter in L-S, as shown in Table 5, could have caused the difference in the DTG curve and have caused a catalytic effect [33, 44]. The lignins were thermally stable below 200 °C, after which they started to degrade, which agreed with previous reports [45]. The higher mass residues of S-A and L-S were attributed to their higher ash contents as seen in Table 5.

The aforementioned lignin characterisations indicated that S-A-P would be the preferred lignin sample for phenol replacement in resins: From the structural compositional analysis, it had the lowest ash and sulphur contents, and a high phenolic hydroxyl content (Table 5). The mid-IR spectra (Figure 2) confirmed

a high hydroxyl content in S-A-P and showed the presence of H-, G-, and S-monomers. From the TGA results (Figure 3**Error! Reference source not found.**), S-A-P was also the most thermally stable, which was attributed to its low ash content (Table 5), and the higher content of G-monomers (Figure 2), with condensed C-C bonds between the monomers that have a very high thermal stability [33].

The preference for the S-A-P lignin was further confirmed with preliminary experiments by making unmodified LPF100_(0,0) resins, synthesised with a NaOH/PL molar ratio of 0.36, and a F/PL molar ratio of 2, with the results shown in Table 7. S-A-P produced a shear strength of 0.430 MPa, which was superior to the shear strengths of 0.280 MPa and 0.145 MPa produced with L-S and L-S-D, respectively. Therefore, further investigations and optimisations were done with the S-A-P lignin only.

Table 7 Shear strength screening experiments using different lignins to make LPF100_(0,0) resins

Resin	Shear strength (MPa)
S-A-P LPF100_(0,0)	0.430 ± 0.026
L-S LPF100_(0,0)	0.280 ± 0.075
L-S-D LPF100_(0,0)	0.145 ± 0.086

3.2 Characterisation of the dried lignin-phenol samples

The suitability of prepared lignin samples for phenol incorporation into chemical structures was tested before LPF synthesis experiments. Such phenol incorporation would be required for phenol substitution levels below 100%, and typically occurs through cleaving of ether bonds and introducing more phenolic hydroxyl groups and reactive sites [9]. The lignin was first reacted with phenol and 2/3 of the NaOH solution and a sample was taken when the reaction was completed, to characterise lignins for structural changes and phenolic hydroxyl content. Figure 4 compares the structural changes to S-A-P after phenolation at a L/P ratio of 68/32.

Changes to the lignin structures as a result of phenolation were as expected, confirming their reactivity and suitability for LPF resin synthesis. The resulting changes in the lignin structure, as required for improved reactivity, were demonstrated with mid-IR spectral analysis (Figure 4): A low wavelength shift occurred from 3366 to 3335 cm^{-1} after phenolation indicating more hydrogen bonds present [46], which was attributed to more phenolic hydroxyl groups present from the phenol incorporated. The phenolic hydroxyl groups are favourable as they allow electrophilic substitutions that direct the hydroxymethyl groups into the *ortho*- or *para*-positions on the aromatic rings [47]. This was further confirmed by the peak at 1215 cm^{-1} becoming more intensive indicating more C-O stretching of phenolic hydroxyl groups [10]. Successful phenol incorporation was seen by the new peak observed at 2750 cm^{-1} from aromatic C-H stretching of new aromatic rings in the phenolated lignin structure [48], a new peak at 754 cm^{-1}, attributed to the linkages formed between the *ortho*- or *para*-positions of phenol, and the α-hydroxyl groups on the

lignin side chain [12]. Another new peak in P-S-A-P was also observed at 692 cm^{-1}, which was assigned to a mono-substituted benzene ring structure that formed [9]. The shoulder band around 1270 cm^{-1} disappeared which indicated that ether bonds were cleaved after the phenolation reaction [9, 49], thereby reducing steric hindrance.

The phenolic hydroxyl contents of dried S-A-P lignin-phenol were determined under different phenolation reaction conditions (Table 1). Increases in the phenolic hydroxyl contents of the lignin-phenol samples of 105% (up to 3.48 mmol/g) and 124% (up to 3.81 mmol/g) at 60% and 80% substitution, respectively, compared to 1.70 mmol/g before phenolation, were observed. The highest phenolic hydroxyl contents of the lignin-phenol were observed at a NaOH/PL molar ratio of 0.378 at both substitution levels and phenolation temperatures of 110 and 80 °C at 60% and 80% substitution, respectively. The higher phenolic hydroxyl content obtained at 60% was expected, as more phenol was added at 60% substitution, compared to 80% substitution, where more lignin was present which had less phenolic hydroxyl groups compared to phenol. The extent of phenol incorporation confirmed the suitability of the selected phenolation conditions for subsequent LPF resin synthesis, through the one-pot phenolation and LPF synthesis method.

Table 1 Phenolic hydroxyl content and pH values of the dried lignin-phenol at 60% and 80% substitution

NaOH/PL molar ratio	Temperature (°C)	Phenolic hydroxyl content (mmol/g sample)		
		Original S-A-P sample 1.70 ± 0.54	60%	80%
0.124	80		3.08	2.01
0.124	110		2.91 [a]	3.31
0.632	80		3.63	2.52 [a]
0.632	110		3.16	2.85
0.124	95		3.55	2.58
0.632	95		3.02	3.05
0.378	80		3.62	3.48 [b]
0.378	110		3.81 [b]	3.16
Centre points:			3.62 ± 0.636	2.89 ± 0.182

[a] Conditions that produced the highest shear strength.

[b] Conditions that produced the highest phenolic hydroxyl content.

3.3 CCD optimisations of the one-pot synthesis

One-pot phenolation and LPF synthesis was applied to the S-A-P lignins, where phenolation and the subsequent LPF synthesis reaction were completely sequentially in the same reaction vessel. This allowed one, integrated experimental design where the phenolation temperature and the NaOH/PL and F/PL molar ratios of the synthesis reaction were varied simultaneously, aiming to maximise the shear strength at each substitution level. At 100 wt% substitution, 0% phenol was incorporated; hence, the LPF synthesis was directly started and no phenolation occurred.

3.3.1 Effect of the substitution level on the shear strength

The shear strengths of the S-A-P LPF100, LPF80 and LPF60 resins obtained from the CCD experiments are shown in Figure 5. According to the GB/T 1473-2013 plywood standard, a shear strength of ≥ 0.70 MPa is required [50], which was attainable at all substitution levels, if favourable reaction conditions were used, as seen in Figure 5. The LPF80 resin performed the best with a maximum shear strength of 1.09 MPa, while the highest shear strengths at 60% and 100% substitution were at 0.987 and 0.786 MPa, respectively. The characterisation of the lignin-phenol after phenolation at 60% and 80% indicated positive changes to the lignin structure (section 3.2) and explained the better performance of the LPF60 and LPF80 resins., compared to the LPF100 resins. Furthermore, no ether bonds were cleaved during the 100% substitution, compare to the phenolation reactions included at 60% and 80% substitutions that cleaved weak ether bonds (Figure 4). LPF80 resin performed better than LPF60 resin, which agreed with previous reports that found that an increase in lignin content lead to better reinforcement structurally up to a point, whereafter it decreased due to the presence of excess lignin that did not form part of the cross-linked network [1, 18, 51].

3.3.2 Effect of the phenolation temperature on the resin shear strength

The highest shear strength of 0.987 MPa at 60% substitution was obtained at phenolation temperatures of 110 °C, as shown in Figure 6a. The highest shear strength of 1.09 MPa at 80% substitution was obtained at phenolation temperatures of 80 °C, as shown in Figure 6b. These temperatures also gave the highest phenolic hydroxyl contents at each respective substitution level (3.48 and 3.81 mmol/g sample), as shown in Table 8.

3.3.3 Effect of NaOH/PL and F/PL molar ratios on resin shear strength

Contour plots describing the effects of NaOH/PL and F/PL molar ratios on the shear strength are shown in Figure 7. The best NaOH/PL and F/PL ratios were 0.124 and 1 for LPF60 and LPF80, as seen in Figure

7a and Figure 7b. These values were lower compared to LPF100 (0.477 and 3 as shown in Figure 7c), and also low compared to previous reports [20, 21, 24, 38]. This was attributed to phenolation causing an apparent increase in reactive sites [9], adding phenolic hydroxyl groups (**Table 1**), and cleaving weak ether bonds (Figure 4), thereby requiring less catalyst and formaldehyde to promote the forward reaction [28]. At too high NaOH/PL ratios side reactions could have occurred: The Cannizzaro reaction where the formaldehyde condenses with itself; therefore, less formaldehyde would be available to react to form large cross-linked structures [19], or the Tollens reaction where the formaldehyde attached to the lignin side chain carbonyl groups instead of the aromatic ring [35].

The highest shear strength of the LPF100 resin was obtained at a NaOH/PL molar ratio of 0.477 and a F/PL molar ratio of 3. The optimum NaOH/PL molar ratio of 0.477 for LPF100 to maximise the shear strength agreed with previous reports using other pulping lignins [1, 18, 24, 52]. The desired F/PL ratio of 3, as seen in Figure 7c, was higher compared to previous reports where ratios between 1.2 and 3 were combined with either substitution levels below 50% [21, 40], or supplementation of the resin with additives during adhesive formulation [22, 24].

3.4 Effect of the reaction conditions for optimisations from the CCD experiments

The shear strength results from the CCD experiments of the one-pot phenolation-synthesis for LPF resin production are shown in Table 9 and Table 10. An ANOVA was done on each CCD to determine if the regression model was statistically significant and to determine which parameters had a significant effect on the shear strength. The ANOVA results, pareto charts and desirability profiles are shown in the supplementary information, where an $\alpha \leq 1$ was assumed to be significant. Although some of the regression models were not statistically significant, they were still used to determine optimums which were then verified experimentally.

Table 9 Shear strength results from the CCD runs with the S-A-P LPF100 resins

NaOH (weight fraction)	F/PL (molar ratio)	Shear strength (MPa) S-A-P LPF100
0.05	1	0.385
0.05	3	0.470
0.22	1	0.172
0.22	3	0.469
0.05	2	0.084
0.135	3	0.661
0.22	2	**0.786**
0.135	1	0.693
0.135	2	0.452
0.135	2	0.443
0.135	2	0.386
0.135	2	0.438
Centre points		0.430 ± 0.026

Table 10 Shear strength results from the CCD runs with the S-A-P LPF80 and LPF60 resins

NaOH (weight fraction)	F/PL (molar ratio)	Temperature (°C)	Shear strength (MPa)	
			S-A-P LPF80	S-A-P LPF60
0.05	1	80	0.930	0.544
0.05	3	80	0.965	0.289
0.05	3	110	0.412	0.647
0.05	1	110	0.916	0.851
0.22	1	80	**1.089**	0.522
0.22	3	80	1.020	0.457
0.22	3	110	0.272	0.333
0.22	1	110	0.369	0.830
0.05	2	95	0.822	0.802
0.135	3	95	0.444	0.107
0.22	2	95	0.855	0.423
0.135	1	95	0.887	**0.987**
0.135	2	80	0.633	0.349
0.135	2	110	0.576	0.575
0.135	2	95	0.511	0.411
0.135	2	95	0.457	0.436
0.135	2	95	0.608	0.444
0.135	2	95	0.462	0.345
0.135	2	95	0.609	
Centre points			0.529 ± 0.067	0.409 ± 0.039

The results from the different CCDs were combined into a regression model to determine the substitution level that would give the highest shear strength. This substitution level was determined to be 68%, with a phenolation temperature of 98.4 °C, a NaOH/PL molar ratio of 0.124, and a F/PL molar ratio of 1. This yielded a shear strength of 1.34 MPa (Equation 1) and was verified experimentally and produced a shear strength of 1.11 ± 0.21 MPa (data not shown). Another regression model was determined from the combined response of the LPF60 and LPF80 CCDs to determine the optimum phenolation temperature at 68% substitution, as shown in Equation 2. The corresponding phenolation temperature was determined to be at 98 °C. These optimum LPF resins that produced the highest shear strength at each substitution level were then characterised further.

Equation 1:

$$\text{Shear strength(MPa)} = -0.312 + 0.0572(68\%) - 0.0005(68\%)^2 - 0.8257(1\frac{F}{PL}) + 0.0576(1\frac{F}{PL})^2 + 0.006(68\% \text{ x } 1\frac{F}{PL}) = 1.34\text{Pa}$$

Equation 2:

$$\text{Shear strength(MPa)} = 0.903\ \text{Mpa} = -5.9753 + 0.0780(\text{LPF\%}) - 2.0889(\frac{NaOH}{PL}) + 21.3173(\text{NaOH/PL})^2 + 0.0848\ (\text{T}) - 0.0001\ (\text{T})^2 - 0.2997(\frac{F}{PL}) + 0.0348(\frac{F}{PL})^2 + 0.0075\ (\text{LPF\% x}\ \frac{NaOH}{PL}) - 0.0008(\text{LPF\% x T}) + 0.0041\ (\text{LPF\% x}\ \frac{F}{PL}) - 0.0508\ (\frac{NaOH}{PL}\ \text{x T}) + 0.1471(\frac{NaOH}{PL}\ \text{x}\ \frac{F}{PL}) - 0.0030\ (\text{T x}\ \frac{F}{PL})$$

∴T=98.4 °C

3.5 LPF resin characterisations

3.5.1 Mid-IR spectra of the LPF resins

Mid-IR spectral analysis was done on a selection of LPF resins as shown in Figure 8. The spectra confirmed that LPF synthesis had occurred during the addition reaction, where formaldehyde is linked onto the free *ortho-* and *para*-positions on the aromatic rings, resulting in a decrease in G-monomers at the shoulder bands at 1272 and 835 cm^{-1} [49, 53].

From the spectral analysis results in Figure 8, it was also observed that cross-linked networks formed during resin synthesis: The bands at 850-750 cm^{-1} indicated tri-substituted benzene rings and confirmed the formation of a cross-linked three-dimensional network structure [40]. The band around 835 cm^{-1} indicated C-H out of plane *para*-substituted benzene, while the bands at 760 cm^{-1} indicated C-H out of plane *ortho*-substituted benzene [49]. Furthermore, the formation of methylene bridges (at 2927, 2850 and 1475-1450 cm^{-1} [49]) showed that formaldehyde attached to the available reactive sites on the phenolated lignin as methylol groups, and then condensed to form methylene bridges and dimethyl ether bridges [17]. Increases in these peak intensities confirmed cross-linking between lignin and/or phenol monomers.

In Figure 9 the absorbances of the methylene peaks (at 1470 cm^{-1}) from the mid-IR spectra of the LPF resins before hot-pressing were plotted against the shear strengths obtained after hot-pressing. The

resins were colour-coded as follows: blue resembled centre point runs of the S-A-P resins, the red and green resembled bad and good performing S-A-P resins with respect to shear strength, respectively. Purple resembled L-S or L-S-D based LPF100_(0,0) resins, and yellow represented S-A or S-A-P LPF68 resins made at optimum conditions (phenolation temperature of 98.4 °C, NaOH/PL molar ratio of 0.124, and F/PL molar ratio of 1). All the resins were made with S-A-P lignin unless otherwise indicated. It was observed that a high methylene bridge content already formed in the resin before hot-pressing, lead to high shear strengths produced after hot-pressing. Therefore, the high shear strength performance of the LPF resins was attributed to a high degree of cross-linking in the resin, while the resins that produced low shear strengths had a low methylene bridge content. This agreed with previous reports concluding that enhanced cross-linking leads to higher adhesive strengths [51, 54].

A principal component analysis (Figure 10) was also done with the mid-IR data (Figure 8), where different clusters were formed by resins that had similar structures. The principal components PC1, PC2, PC3, and PC4 were found to describe 61.4%, 16.1%, 9.2% and 4.4% of the variability in the data, respectively. By comparing the mid-IR data of the resins, the following peaks were identified that caused the resins to cluster together: total hydroxyl groups (3400-3200 cm^{-1}), G-monomers (1272 and 835 cm^{-1}), methylene bridges (1470 cm^{-1}) and ether bridges (1150-1050 cm^{-1}). Cluster A was separated due to its high total hydroxyl content (3400-3200 cm^{-1}) and high methylene bridge content (1470 cm^{-1}. Cluster B containing S-A-P LPF80_(0,0,0) had a high total hydroxyl content and had an overlap of the two peaks at 987 and 1030 cm^{1}, which indicated the presence of C-O vibration of ether bands [55]. Cluster C had no G-monomers (1272 or 835 cm^{-1}) and a low degree of cross-linking, with low absorbances for methylene (1470 cm^{-1}) or dimethyl ether peaks (1150-1050 cm^{-1}). Cluster D had G-monomers present at 1279 cm^{-1}, indicating more reactive sites available for cross-linking. Cluster E contained the two samples with the lowest total hydroxyl group content (3400-3200 cm^{-1}) namely LPF100_(1,-1) and LPF80_(-1,1,-1). Cluster G had the highest methylene bridge (1470 cm^{-1}) content and indicated G-monomers (1279 cm^{-1}). The relationships between these spectral properties and resin performances could subsequently be deduced.

Methylene bridges are very strong C-C bonds [56], where the formation of these bonds before the curing reaction indicated that cross-linking already occurred to some extent, which would be favourable if these cross-linked networks were successfully embedded into the plywood [50]. This was confirmed by the high content in clusters G and A which yielded high shear strengths (Figure 10). In contrast cluster E had few methylene bridges and produced a low shear strength (Figure 10). Ether bonds formed during the condensation of methylol groups also indicated that cross-linking occurred [24]. This high degree of cross-linking would then lead to a more thermally stable resin [20] and yield a higher adhesive strength [51]. A high hydroxyl content in the LPF resins before curing would be favourable for further cross-linking to occur, which was seen in clusters A and B. In contrast, cluster E had the lowest total hydroxyl content and low shear strengths (Figure 10). The presence of G-monomers indicated that a reactive site was still available for methylol to react with to form a methylene bridge, which also contributed to the high shear strength in cluster G. Furthermore, a decrease in G-monomers could have indicated that successful addition of formaldehyde happened at the reactive site, or that cross-linking

occurred during the condensation reaction. Cluster C had no G-monomers (1272 or 835 cm^{-1}) and a low degree of cross-linking, which could indicate that addition at the available reactive sites was successful for the LPF100 resins, but further cross-linking did not occur which could be attributed to the presumed higher steric hindrance at 100% substitution. Cluster D had G-monomers present at 1279 cm^{-1}, indicating more reactive sites available for cross-linking.

3.5.2 TGA of the LPF resins

Degradation of the LPF resins occurred in three steps, namely post-curing (200 to 300 °C), thermal reforming (300 to 500 °C), and ring stripping (500 to 600 °C) [57]. Greater thermal stability and less mass loss in the TGA curves (Figure 11) indicates greater network formation in the resins [51], where a high degree of cross-linking could lead to high shear strengths (Figure 10). The peak at 450 °C was attributed to methylene bridges formed [20], where a higher frequency of these strong methylene bridges that are more resistant to thermal degradation was favourable for LPF resins, as the higher degree of cross-linking contributed to a high shear strength and thermal stability of the resin if the lignin macromolecule was successfully embedded [54]. Only a small peak was observed for LPF100_(1,0) around 450 °C which indicated that not a lot of methylene bridges formed [20], compared to the other resins. This agreed with the findings from Figure 10, where many methylene bridges present in the mid-IR data at 1470 cm^{-1} correlated with a high shear strength in the LPF resins, which was then also supported by a high methylene bridge peak around 450 °C in the DTG curve.

LPF68_(optimum) was found to be the most thermally stable as it had the highest maximum thermal degradation at 382 °C, and it also had the highest weight residue throughout. It also had the highest shear strength (Figure 9). LPF60_(0,-1,0) also showed good thermal stability, with its highest maximum thermal degradation at 367 °C, followed by LPF80_(1,-1,-1) at 343 °C and then LPF100_(1,0) at 264°C. LPF100_(1,0) had a high thermal degradation peak around 270 °C, while there was not a lot of weight loss in the resins at lower substitution levels, which could be explained by the phenolation reaction that already cleaved weak bonds (Figure 4) which degrade at lower temperatures.

3.5.Free formaldehyde contents and pH values of the LPF resins

At the most favourable operating conditions, high shear strengths and low free formaldehyde contents were produced. A shear strength of 0.70 MPa, free formaldehyde content below 0.30 wt% and pH value above 7 is required by the GB/T 1473-2013 standard [50]. The pH value and free formaldehyde content was determined at each substitution level for the resin that gave the highest shear strength, and for the resin made at centre point conditions.

The resins that produced the highest shear strengths at each substitution level, had the lowest free formaldehyde content, as shown in Table 11. These were LPF100_(1,0), LPF80_(1,-1,0), LPF60_(0,-1,1), and LPF68_(optimum), with free formaldehyde contents of 0.298%, 0.117%, 0.178%, and 0.284%.

Standard deviations for the free formaldehyde contents ranged between 0.002 wt% and 0.033 wt%. This verified that at the best reaction conditions of that tested, most of the formaldehyde reacted and attached to the phenolic lignin structures, leaving a low residual formaldehyde content.

In contrast, at the centre points the LPF80_(0,0,0) and LPF60_(0,0,0) resins failed to adhere to the free formaldehyde standard, indicating that the conditions were not favourable for most of the formaldehyde to react, leading to a high free formaldehyde content, as shown in Table 11. These resins did not show G-monomer peaks in their mid-IR spectra at 835 cm^{-1} (shown in supplementary material), which showed that there were limited reactive sites for the residual formaldehyde to attach during the addition reaction, resulting in a high free formaldehyde content, while a G-monomer peak was observed for the LPF100_(0,0) resin. These resins also showed small overtone peaks at 2724 cm^{-1}, attributed to the C-H bending in formaldehyde [24], indicating unreacted formaldehyde present.

Table 11 Free formaldehyde contents, shear strength, and pH values of the centre point and highest shear strength LPF resins, at each substitution level

	Resin ID	Free CH_2O (wt%)	pH value	Shear strength (MPa)
Highest shear strength	LPF100_(1,0)	0.298	9.9	0.786
	LPF80_(1,-1,0)	0.117	11.4	1.09
	LPF60_(0,-1,1)	0.178	10.5	0.987
	LPF68_(optimum)	0.284	9.0	1.11
Centre points runs	LPF100_(0,0)	0.291	9.1	0.430
	LPF80_(0,0,0)	0.837	10.4	0.529
	LPF60_(0,0,0)	0.554	10.4	0.409

3.5.4 Performance evaluation of the resin in particleboard manufacture

The optimum S-A-P LPF68_(optimum) resin had sufficient performance to result in particleboard with acceptable resistance to moisture and also confirmed the shear strength performances as observed with the plywood. This resin produced better particleboard at higher lignin substitution levels compared to those reported previously for LPF resins [2, 58, 59]. The particleboards were produced and tested according to the ASTM D1037-12 standard, and the results were tabulated in Table 12. The ANSI A208.1-1999 standard for high-density (> 800 kg/m^3) particleboards specifies a MOR ≥ 23.5 MPa and MOE ≥ 2750 MPa. The particleboard made with LPF68_(optimum) exceeded these MOR and MOE specifications. A MOR and MOE of 40 and 3209 MPa were obtained, respectively. The TS and WA were low and determined to be 13.5% and 37.2%, respectively. Another board was made with commercial Bondtite (a

urea-based resin used for interior application) mixed with hexamine as a cross-linker, used only as a reference board. The MOR and MOE of the reference board was lower as expected at 27 and 3592 MPa, respectively. The TS and WA were determined to be 61.8% and 73.3%, respectively; where the lower moisture resistance of this urea-based resin was expected [60].

Table 12 Characteristic results of particleboard produced with LPF68 and Bondtite

	Moisture in dried boards (%)	Density (kg/m^3)	Thickness (mm)	TS (%)	WA (%)	MOR (MPa)	MOE (MPa)
LPF68	8.41	0.915	5.93	13.5	37.2	40	3209
Bondtite	10.9	0.867	5.90	61.8	73.3	27	3592

Conclusions

Purified soda lignin had a higher reactivity and less impurities compared to impure soda lignin and lignosulphonate and foreshadowed to be the most promising replacement for phenol in resin synthesis. A one-pot method from literature was used for the first time with an industrial pulping lignin, which allowed a direct transition from the phenolation to LPF synthesis in alkaline conditions, in one reaction vessel. The best phenolation temperatures were determined to be at 110 and 80 °C at 60% and 80% substitution, respectively. The best synthesis reaction conditions for 60% and 80% substitution were at a NaOH/PL molar ratio of 0.124 and a F/PL molar ratio of 1, which was lower compared to previous reports. At 100% substitution without any lignin modification, the optimum NaOH/PL molar ratio was 0.477, which corresponded to previous reports, while the best F/PL molar ratio in the tested range was at 3, which was higher than expected based on previous reports, and was attributed to the high incorporation of the less reactive soda lignin.

The highest shear strength attained from the CCD runs was with LPF80 (1.09 MPa), which performed better than LPF60 (0.987 MPa) and LPF100 (0.786 MPa), governed by 80% substitution having a favourable degree of branched lignin monomers, while still having a high enough reactivity to form cross-linked networks. The highest attainable shear strength was 1.11 MPa, at 68% substitution as determined by regression models, at a phenolation temperature of 98.4 °C, NaOH/PL molar ratio of 0.124, and F/PL molar ratio of 1. A high shear strength performance at favourable reaction conditions tested was attributed to a high degree of cross-linking that occurred, which was confirmed by a high thermal stability and a high methylene bridge formation before the final curing reaction.

The performance of this soda lignin as a LPF resin was further confirmed by strength results obtained when tested in particleboard manufacture giving a MOR and MOE of 23.5 MPa and 2750 MPa, respectively, which adhered to the ANSI A208.1-1999 standard. It also proved acceptable resistance to water absorption (37.2%) and thickness swelling (13.5%). This unclean pulping lignin is unique in its

properties and was the first lignin to produce LPF resins at 100% substitution without modification or additives while adhering to plywood standard specifications.

Declarations

Acknowledgements: The authors would like to thank the Paper Manufacturers Association of South Africa (PAMSA) in conjunction with Sappi Southern Africa Ltd for the scholarship received by the first author.

Availability of data and material: The resulting data from the study are available from the corresponding author upon request.

References

1. Khan, M.A., Ashraf, S.M., Malhotra, V.P.: Eucalyptus bark lignin substituted phenol formaldehyde adhesives: A study on optimization of reaction parameters and characterization. J. Appl. Polym. Sci. **92**, 3514–3523 (2004). https://doi.org/10.1002/app.20374
2. Çetin, N.S., Özmen, N.: Use of organosolv lignin in phenol-formaldehyde resins for particleboard production: I. Organosolv lignin modified resins. Int J Adhes Adhes. **22**, 477–480 (2002). https://doi.org/10.1016/S0143-7496(02)00058-1
3. Klašnja, B., Kopitović, S.: Lignin-Phenol-Formaldehyde resins as adhesives in the production of plywood. Holz als Roh- und Werkst. **50**, 282–285 (1992). https://doi.org/10.1007/BF02615352
4. Tang, Q., Qian, Y., Yang, D., et al.: Lignin-based nanoparticles: A review on their preparations and applications. Polymers (Basel). **12**, 1–22 (2020). https://doi.org/10.3390/polym12112471
5. Tejado, A., Peña, C., Labidi, J., et al.: Physico-chemical characterization of lignins from different sources for use in phenol-formaldehyde resin synthesis. Bioresour. Technol. **98**, 1655–1663 (2007). https://doi.org/10.1016/j.biortech.2006.05.042
6. El Mansouri, N.E., Farriol, X., Salvadó, J.: Structural modification and characterization of lignosulfonate by a reaction in an alkaline medium for its incorporation into phenolic resins. J. Appl. Polym. Sci. **102**, 3286–3292 (2006). https://doi.org/10.1002/app.24744
7. Hon, D.N.S.: Chemical modification of lignocellulosic materials. CRC Press (1996)
8. Hu, L., Pan, H., Zhou, Y., et al.: Methods to improve lignin's reactivity as a phenol substitute and as replacement for other phenolic compounds: A brief review. BioResources. **6**, 3515–3525 (2011). https://doi.org/10.15376/biores.6.3.3515-3525
9. Zhao, M., Jing, J., Zhu, Y., et al.: Preparation and performance of lignin-phenol-formaldehyde adhesives. Int J Adhes Adhes. **64**, 163–167 (2016). https://doi.org/10.1016/j.ijadhadh.2015.10.010
10. Ghorbani, M., Konnerth, J., van Herwijnen, H.W.G., et al.: Commercial lignosulfonates from different sulfite processes as partial phenol replacement in PF resole resins. J. Appl. Polym. Sci. **135**, 1–11 (2018). https://doi.org/10.1002/app.45893

11. Thébault, M., Kutuzova, L., Jury, S., et al.: Effect of phenolation, lignin-type and degree of substitution on the properties of lignin-modified phenol-formaldehyde impregnation resins: Molecular weight distribution, wetting behavior, rheological properties and thermal curing profiles. J Renew Mater. **8**, 603–630 (2020). https://doi.org/10.32604/jrm.2020.09616
12. Alonso, M.V., Oliet, M., Rodríguez, F., et al.: Modification of ammonium lignosulfonate by phenolation for use in phenolic resins. Bioresour. Technol. **96**, 1013–1018 (2005). https://doi.org/10.1016/j.biortech.2004.09.009
13. Karthäuser, J., Biziks, V., Mai, C., Militz, H.: Lignin and Lignin-Derived Compounds for Wood Applications—A. Review. Molecules. **26**, 2533 (2021). https://doi.org/10.3390/molecules26092533
14. Jiang, X., Liu, J., Du, X., et al.: Phenolation to Improve Lignin Reactivity toward Thermosets Application. ACS Sustain Chem Eng. **6**, 5504–5512 (2018). https://doi.org/10.1021/acssuschemeng.8b00369
15. Lee, W., Chang, K.-C., Tseng, I.-M.: (2011) Properties of phenol-formaldehyde resins prepared from phenol-liquefied lignin. J. Appl. Polym. Sci. 124:n/a-n/a. https://doi.org/10.1002/app.35539
16. Gan, L., Pan, X.: Phenol-Enhanced Depolymerization and Activation of Kraft Lignin in Alkaline Medium. Ind. Eng. Chem. Res. **58**, 7794–7800 (2019). https://doi.org/10.1021/acs.iecr.9b01147
17. Yang, S., Wen, J.-L., Yuan, T.-Q., Sun, R.-C.: Characterization and phenolation of biorefinery technical lignins for lignin–phenol–formaldehyde resin adhesive synthesis. RSC Adv. **4**, 57996–58004 (2014). https://doi.org/10.1039/C4RA09595B
18. Abdelwahab, N.A., Nassar, M.A.: Preparation, optimisation and characterisation of lignin phenol formaldehyde resin as wood adhesive. Pigment Resin Technol. **40**, 169–174 (2011). https://doi.org/10.1108/03699421111130432
19. Sarkar, S., Adhikari, B.: Lignin-modified phenolic resin: Synthesis optimization, adhesive strength, and thermal stability. J. Adhes. Sci. Technol. **14**, 1179–1193 (2000). https://doi.org/10.1163/156856100743167
20. Zhang, W., Ma, Y., Wang, C., et al.: Preparation and properties of lignin-phenol-formaldehyde resins based on different biorefinery residues of agricultural biomass. Ind Crops Prod. **43**, 326–333 (2013). https://doi.org/10.1016/j.indcrop.2012.07.037
21. Ghorbani, M., Liebner, F., van Herwijnen, H.W.G., et al.: Lignin phenol formaldehyde resoles: The impact of lignin type on adhesive properties. BioResources. **11**, 6727–6741 (2016). https://doi.org/10.15376/biores.11.3.6727-6741
22. Kalami, S., Chen, N., Borazjani, H., Nejad, M.: Comparative analysis of different lignins as phenol replacement in phenolic adhesive formulations. Ind Crops Prod. **125**, 520–528 (2018). https://doi.org/10.1016/j.indcrop.2018.09.037
23. Kalami, S., Arefmanesh, M., Master, E., Nejad, M.: Replacing 100% of phenol in phenolic adhesive formulations with lignin. J. Appl. Polym. Sci. **134**, 45124 (2017). https://doi.org/10.1002/app.45124
24. Govender, P., Majeke, B.M., Alawode, A.O., et al.: The use of south african spent pulping liquor to synthesize lignin phenol-formaldehyde resins. For Prod J. **70**, 503–511 (2020).

https://doi.org/10.13073/FPJ-D-20-00047

25. Yaakob, M.N.A., Bin Roslan, R., Salim, N., Zakaria, S.: Comparison of Phenol-Formaldehyde and Lignin-Formaldehyde Resin Adhesives for Wood Application. Mater Sci Forum. **1025**, 307–311 (2021). https://doi.org/10.4028/www.scientific.net/msf.1025.307
26. García, A., Toledano, A., Serrano, L., et al.: Characterization of lignins obtained by selective precipitation. Sep Purif Technol. **68**, 193–198 (2009). https://doi.org/10.1016/j.seppur.2009.05.001
27. Areskogh, D., Li, J., Gellerstedt, G., Henriksson, G.: Investigation of the molecular weight increase of commercial lignosulfonates by laccase catalysis. Biomacromol. **11**, 904–910 (2010). https://doi.org/10.1021/bm901258v
28. Siddiqui, H., Mahmood, N., Yuan, Z., et al.: Sustainable bio-based phenol-formaldehyde resoles using hydrolytically depolymerized kraft lignin. Molecules. **22**, 1–19 (2017). https://doi.org/10.3390/molecules22111850
29. Huang, Z., Wang, N., Zhang, Y., et al.: Effect of mechanical activation pretreatment on the properties of sugarcane bagasse/poly(vinyl chloride) composites. Compos Part A Appl Sci Manuf. **43**, 114–120 (2012). https://doi.org/10.1016/j.compositesa.2011.09.025
30. Alawode, A.O.O., Bungu, P.S.S.E.E., Amiandamhen, S.O.O., et al.: Properties and characteristics of novel formaldehyde-free wood adhesives prepared from Irvingia gabonensis and Irvingia wombolu seed kernel extracts. Int J Adhes Adhes. **95**, 102423 (2019). https://doi.org/10.1016/j.ijadhadh.2019.102423
31. Khokarale, S.G., Le-that, T., Mikkola, J.: (2016) Carbohydrate Free Lignin: A Dissolution – Recovery Cycle of Sodium Lignosulfonate in a Switchable Ionic Liquid System. ACS Sustain Chem Eng 4:. https://doi.org/10.1021/acssuschemeng.6b01927
32. Marques, A.P., Evtuguin, D.V., Magina, S., et al.: Chemical composition of Spent liquors from acidic magnesium-based Sulphite pulping of Eucalyptus globulus. J Wood Chem Technol. **29**, 322–336 (2009). https://doi.org/10.1080/02773810903207754
33. Naron, D.R., Collard, F.X., Tyhoda, L., Görgens, J.F.: Characterisation of lignins from different sources by appropriate analytical methods: Introducing thermogravimetric analysis-thermal desorption-gas chromatography–mass spectroscopy. Ind Crops Prod. **101**, 61–74 (2017). https://doi.org/10.1016/j.indcrop.2017.02.041
34. Doherty, W.O.S., Mousavioun, P., Fellows, C.M.: Value-adding to cellulosic ethanol: Lignin polymers. Ind Crops Prod. **33**, 259–276 (2011). https://doi.org/10.1016/j.indcrop.2010.10.022
35. Matsushita, Y.: Conversion of technical lignins to functional materials with retained polymeric properties. J Wood Sci. **61**, 230–250 (2015). https://doi.org/10.1007/s10086-015-1470-2
36. Podschun, J., Stücker, A., Saake, B., Lehnen, R.: Structure-function relationships in the phenolation of lignins from different sources. ACS Sustain Chem Eng. **3**, 2526–2532 (2015). https://doi.org/10.1021/acssuschemeng.5b00705
37. Taverna, M.E., Felissia, F., Area, M.C., et al.: Hydroxymethylation of technical lignins from South American sources with potential use in phenolic resins. J. Appl. Polym. Sci. **136**, 47712 (2019).

https://doi.org/10.1002/app.47712

38. Moubarik, A., Grimi, N., Boussetta, N., Pizzi, A.: Isolation and characterization of lignin from Moroccan sugar cane bagasse: Production of lignin-phenol-formaldehyde wood adhesive. Ind Crops Prod. **45**, 296–302 (2013). https://doi.org/10.1016/j.indcrop.2012.12.040
39. Li, J.J., Wang, W., Zhang, S., et al.: Preparation and characterization of lignin demethylated at atmospheric pressure and its application in fast curing biobased phenolic resins. RSC Adv. **6**, 67435–67443 (2016). https://doi.org/10.1039/c6ra11966b
40. El Mansouri, N.-E., Qiaolong, Y., Huang, F.: Preparation and Characterization of Phenol-Formaldehyde Resins Modified with Alkaline Rice Straw Lignin. BioResources. **13**, 8061–8075 (2018). https://doi.org/10.15376/biores.13.4.8061-8075
41. Wen, J.L., Xue, B.L., Xu, F., Sun, R.C.: Unveiling the Structural Heterogeneity of Bamboo Lignin by In Situ HSQC NMR Technique. Bioenergy Res. **5**, 886–903 (2012). https://doi.org/10.1007/s12155-012-9203-5
42. Yang, H., Xie, Y., Zheng, X., et al.: Comparative study of lignin characteristics from wheat straw obtained by soda-AQ and kraft pretreatment and effect on the following enzymatic hydrolysis process. Bioresour. Technol. **207**, 361–369 (2016). https://doi.org/10.1016/j.biortech.2016.01.123
43. Boeriu, C.G., Bravo, D., Gosselink, R.J.A., Van Dam, J.E.G.: Characterisation of structure-dependent functional properties of lignin with infrared spectroscopy. Ind Crops Prod. **20**, 205–218 (2004). https://doi.org/10.1016/j.indcrop.2004.04.022
44. Majeke, B.M., Collard, F.X., Tyhoda, L., Görgens, J.F.: (2021) The synergistic application of quinone reductase and lignin peroxidase for the deconstruction of industrial (technical) lignins and analysis of the degraded lignin products. Bioresour. Technol. 319:. https://doi.org/10.1016/j.biortech.2020.124152
45. Nsaful, F., Collard, F.X., Carrier, M., et al.: Lignocellulose pyrolysis with condensable volatiles quantification by thermogravimetric analysis - Thermal desorption/gas chromatography-mass spectrometry method. J Anal Appl Pyrolysis. **116**, 86–95 (2015). https://doi.org/10.1016/j.jaap.2015.10.002
46. Ma, Y., Zhao, X., Chen, X., Wang, Z.: An approach to improve the application of acid-insoluble lignin from rice hull in phenol-formaldehyde resin. Colloids Surfaces A Physicochem Eng Asp. **377**, 284–289 (2011). https://doi.org/10.1016/j.colsurfa.2011.01.006
47. Ghorbani, M., Konnerth, J., Budjav, E., et al.: Ammoxidized Fenton-Activated Pine Kraft Lignin Accelerates Synthesis and Curing of Resole Resins. Polymers (Basel). **9**, 43 (2017). https://doi.org/10.3390/polym9020043
48. Taleb, F., Ammar, M., Mosbah, M., ben, et al.: Chemical modification of lignin derived from spent coffee grounds for methylene blue adsorption. Sci Rep. **10**, 1–13 (2020). https://doi.org/10.1038/s41598-020-68047-6
49. Hussin, M.H., Han Zhang, H., Aziz, N.A., et al.: Preparation of environmental friendly phenol-formaldehyde wood adhesive modified with kenaf lignin. Beni-Suef Univ J Basic Appl Sci. **6**, 409–

418 (2017). https://doi.org/10.1016/j.bjbas.2017.06.004

50. Yang, S., Zhang, Y., Yuan, T.Q., Sun, R.C.: Lignin-phenol-formaldehyde resin adhesives prepared with biorefinery technical lignins. J. Appl. Polym. Sci. **132**, 1–8 (2015). https://doi.org/10.1002/app.42493
51. Khan, M.A., Ashraf, S.M.: Studies on thermal characterization of lignin: Substituted phenol formaldehyde resin as wood adhesives. J. Therm. Anal. Calorim. **89**, 993–1000 (2007). https://doi.org/10.1007/s10973-004-6844-4
52. Alonso, M.V., Oliet, M., Rodríguez, F., et al.: Use of a methylolated softwood ammonium lignosulfonate as partial substitute of phenol in resol resins manufacture. J. Appl. Polym. Sci. **94**, 643–650 (2004). https://doi.org/10.1002/app.20887
53. Wang, G., Chen, H.: Carbohydrate elimination of alkaline-extracted lignin liquor by steam explosion and its methylolation for substitution of phenolic adhesive. Ind Crops Prod. **53**, 93–101 (2014). https://doi.org/10.1016/j.indcrop.2013.12.020
54. Pang, B., Yang, S., Fang, W., et al.: Structure-property relationships for technical lignins for the production of lignin-phenol-formaldehyde resins. Ind Crops Prod. **108**, 316–326 (2017). https://doi.org/10.1016/j.indcrop.2017.07.009
55. Alonso, M.V., Rodrguez, J.J., Oliet, M., et al.: Characterization and structural modification of ammonic lignosulfonate by methylolation. J. Appl. Polym. Sci. **82**, 2661–2668 (2001). https://doi.org/10.1002/app.2119
56. Dunky, M.: Adhesives in the Wood Industry. In: Handbook of Adhesive Technology, Revised and Expanded. CRC Press (2003)
57. Yang, W., Rallini, M., Natali, M., et al.: Preparation and properties of adhesives based on phenolic resin containing lignin micro and nanoparticles: A comparative study. Mater Des. **161**, 55–63 (2019). https://doi.org/10.1016/j.matdes.2018.11.032
58. Iwakiri, V.T., Trianoski, R., Razera, D.L., et al.: (2019) Production of Structural Particleboard of Mimosa Scabrella Benth With Lignin Phenol-formaldehyde Resin. Floresta e Ambient 26:. https://doi.org/10.1590/2179-8087.100617
59. Stücker, A., Schütt, F., Saake, B., Lehnen, R.: Lignins from enzymatic hydrolysis and alkaline extraction of steam refined poplar wood: Utilization in lignin-phenol-formaldehyde resins. Ind Crops Prod. **85**, 300–308 (2016). https://doi.org/10.1016/j.indcrop.2016.02.062
60. Mamza, P.A.P., Ezeh, E.C., Gimba, E.C., Arthur, D.E.: Comparative Study Of Phenol Formaldehyde And Urea Formaldehyde Particleboards From Wood Waste For Sustainable Environment. Int J Sci Technol Res **3**, 53–56 (2014)

Figures

Figure 1

Experimental setup used for the one-pot phenolation and LPF synthesis

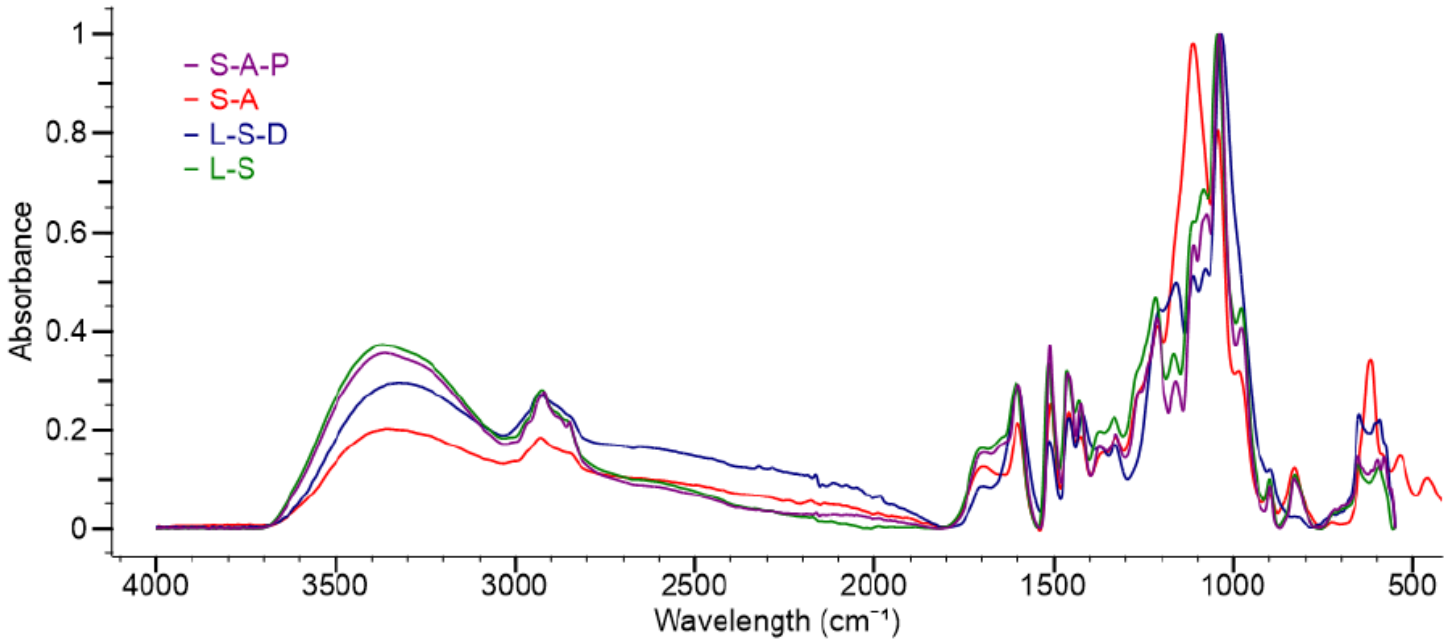

Figure 2

Mid-IR spectra of the different lignin samples

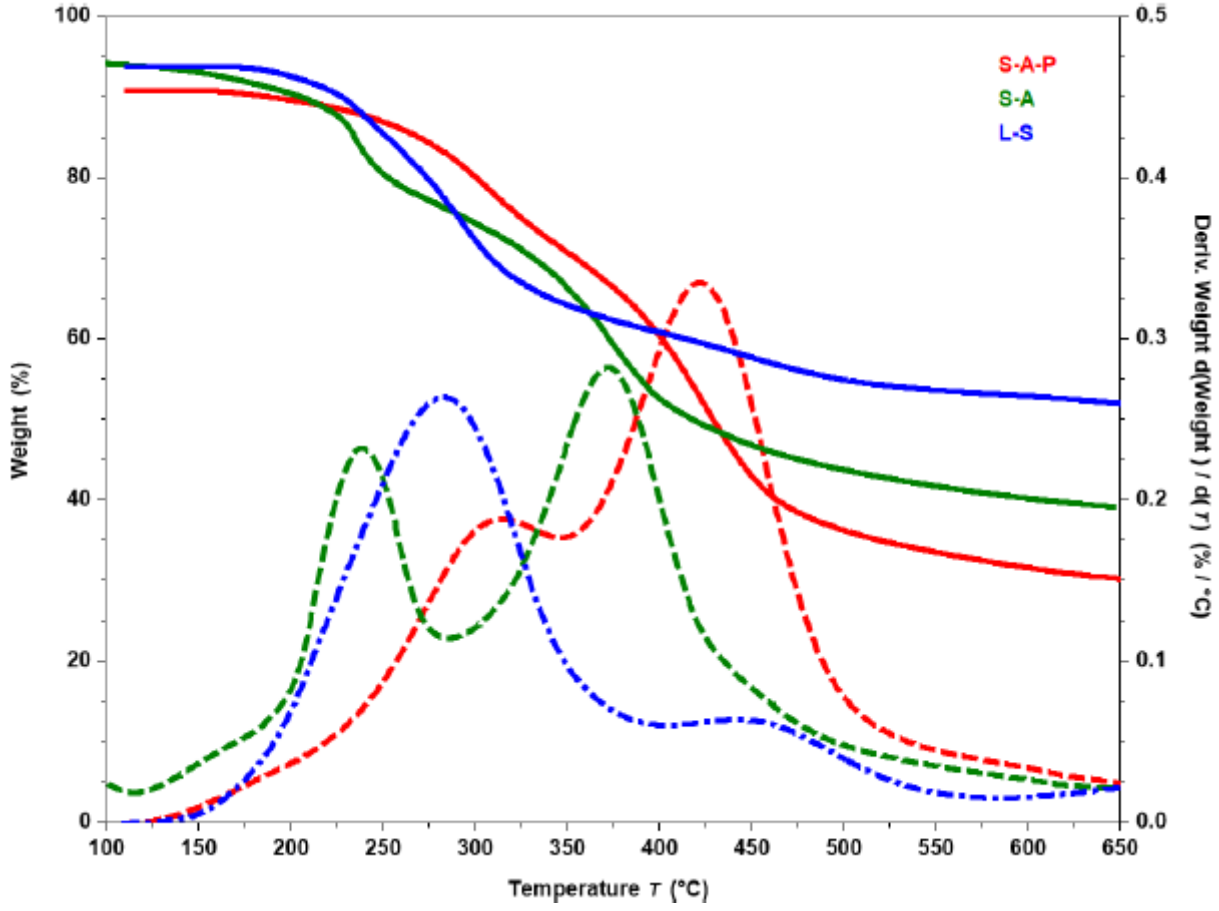

Figure 3

TGA and DTG curves of the lignin samples

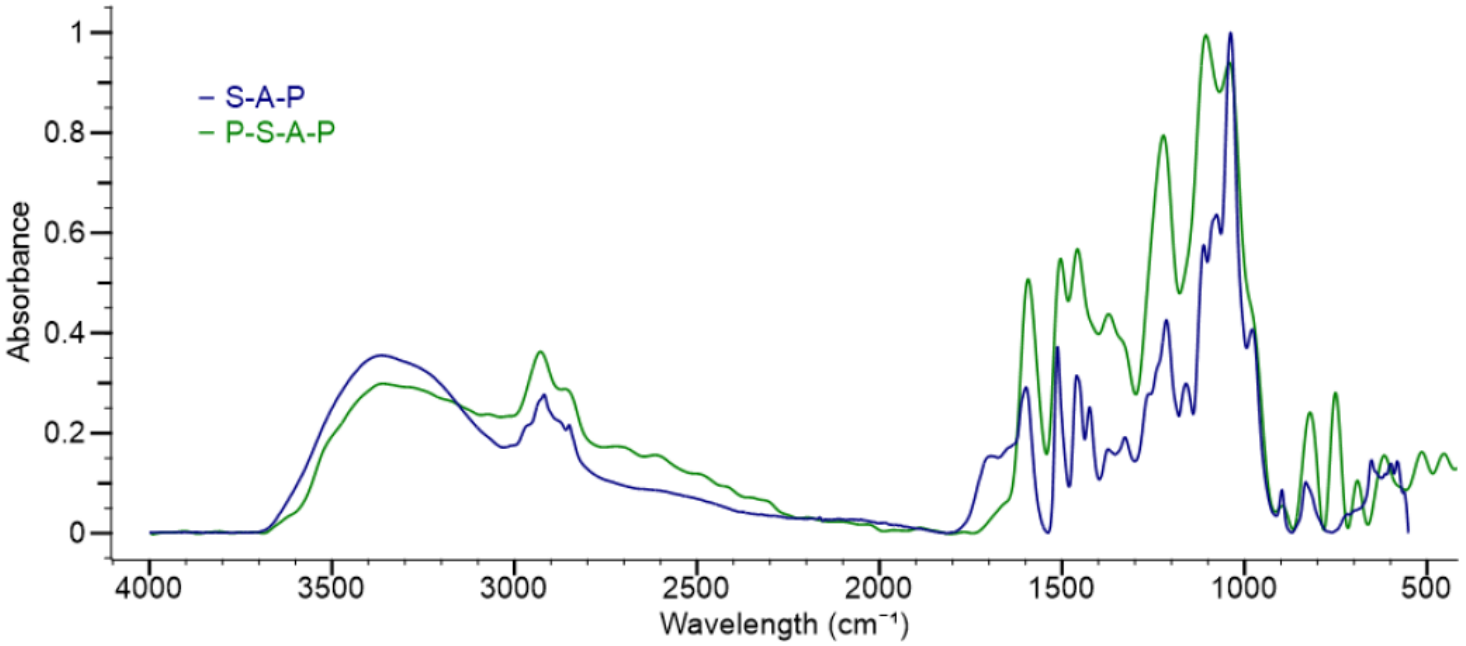

Figure 4

The mid-IR spectra of the purified soda lignin before and after phenolation

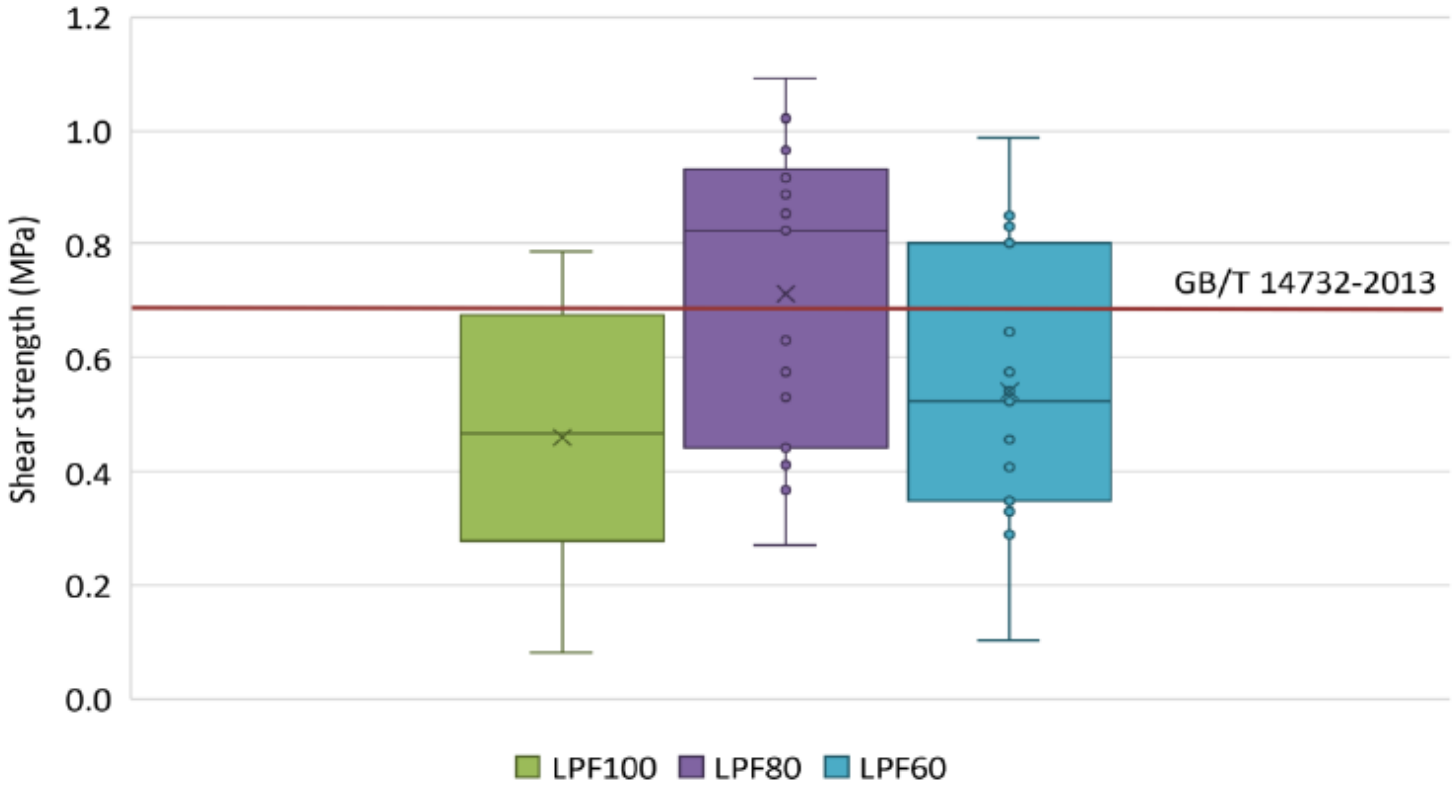

Figure 5

Shear strengths obtained from each CCD at 60%, 80%, and 100% substitution

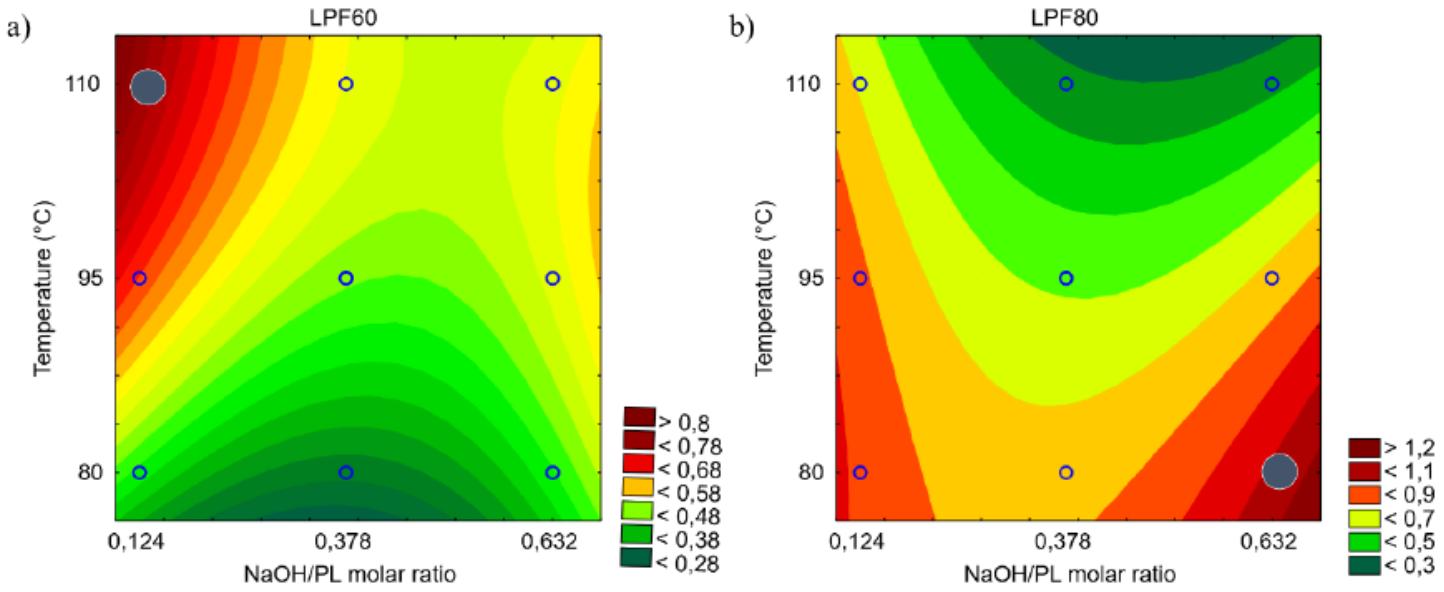

Figure 6

Contour plots of the effect of the NaOH/PL ratio and phenolation reaction temperature on the shear strength of the LPF60 resins (a) and LPF80 resins (b)

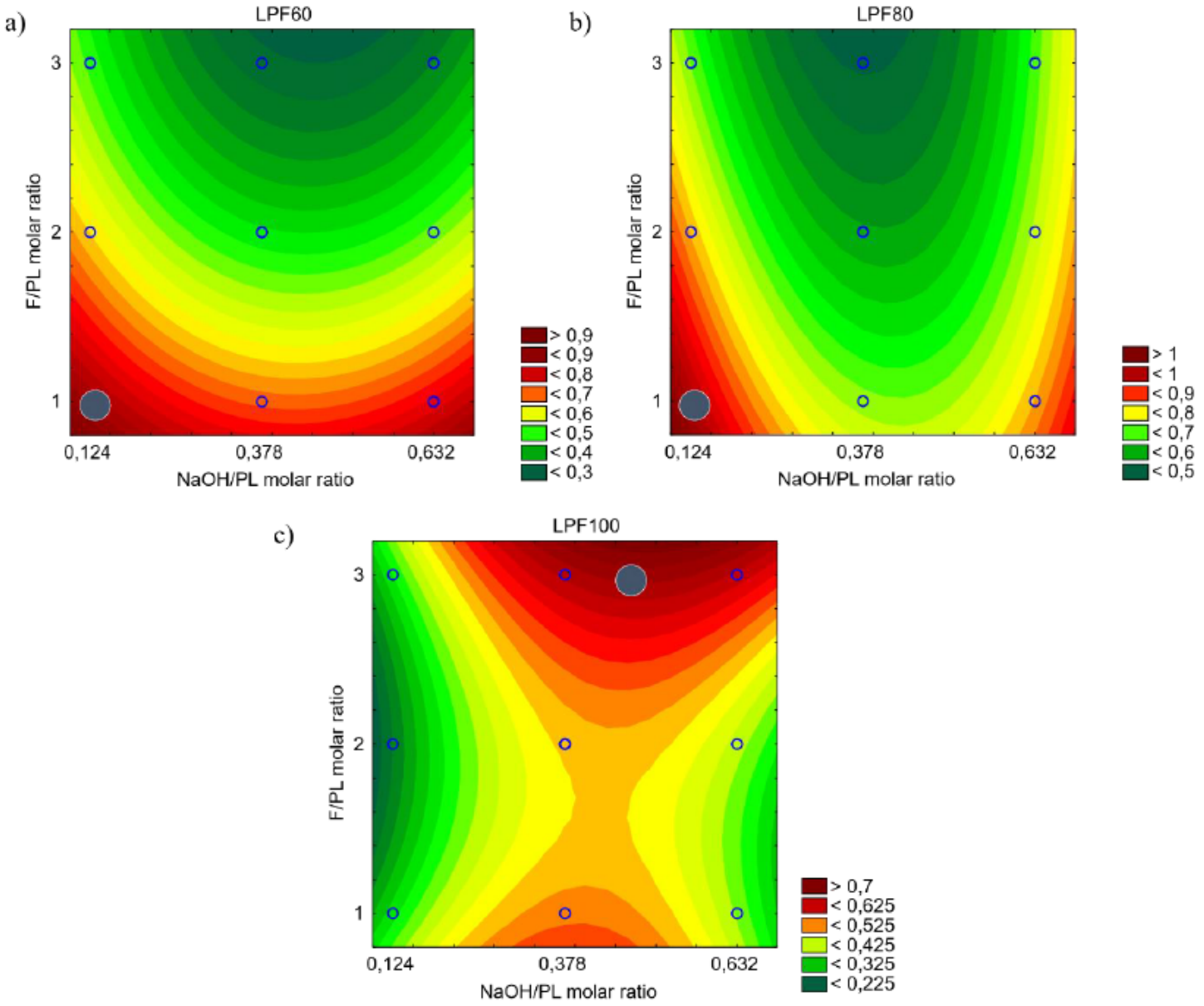

Figure 7

Contour plots showing the effect of the F/PL ratio and the NaOH/PL ratio on the shear strength for each CCD: LPF60 (a), LPF80 (b) and LPF100 (c)

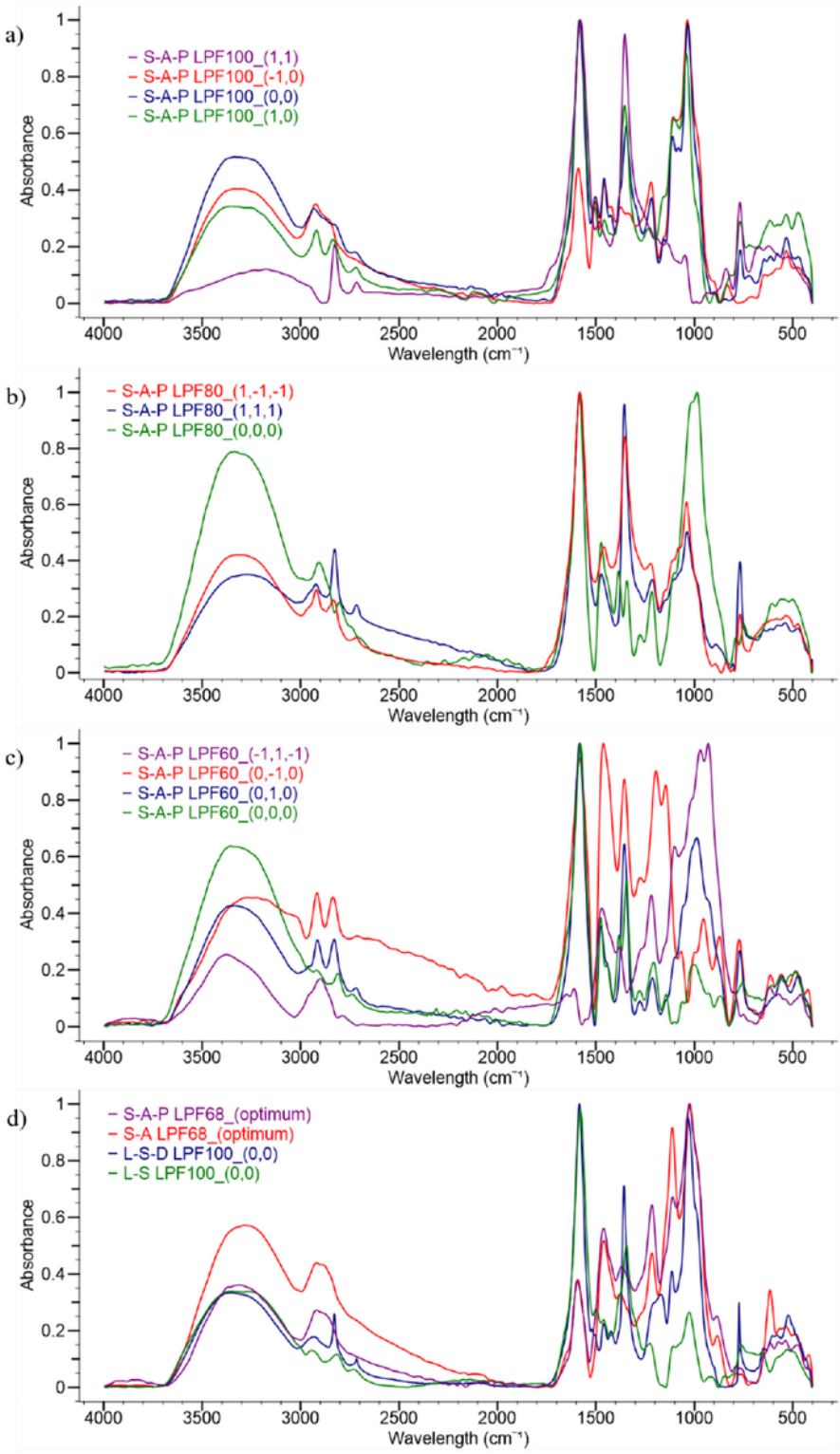

Figure 8

Mid-IR spectra of the resins at different substitution levels (a) LPF100, (b) LPF80, (c) LPF60, (d) L-S and L-S-D LPF100 resins, and S-A and S-A-P LPF68 resins

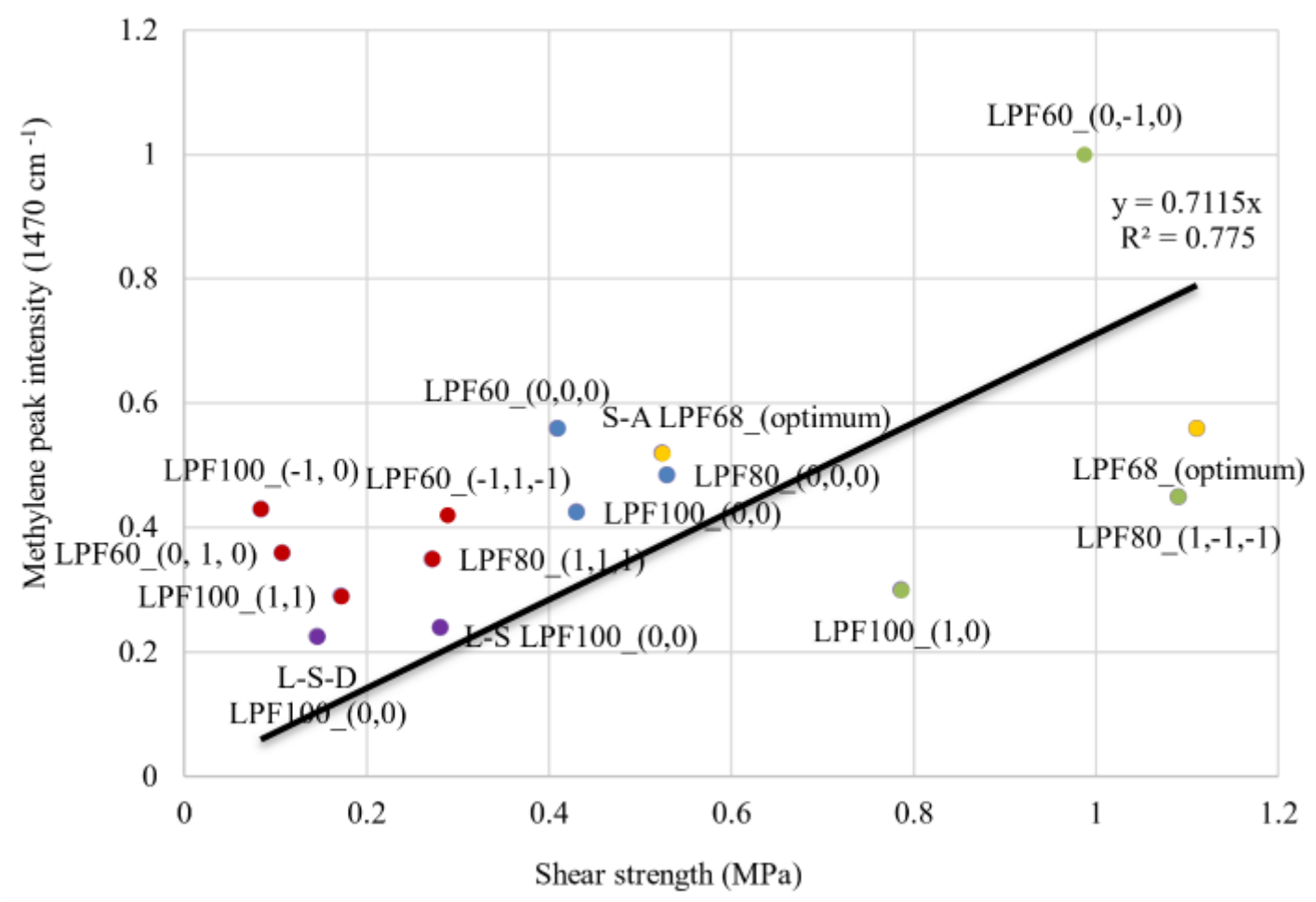

Figure 9

Scatter plot correlating the methylene bridges formed at 1470 cm-1 from the mid-IR data to the shear strength of the LPF resins

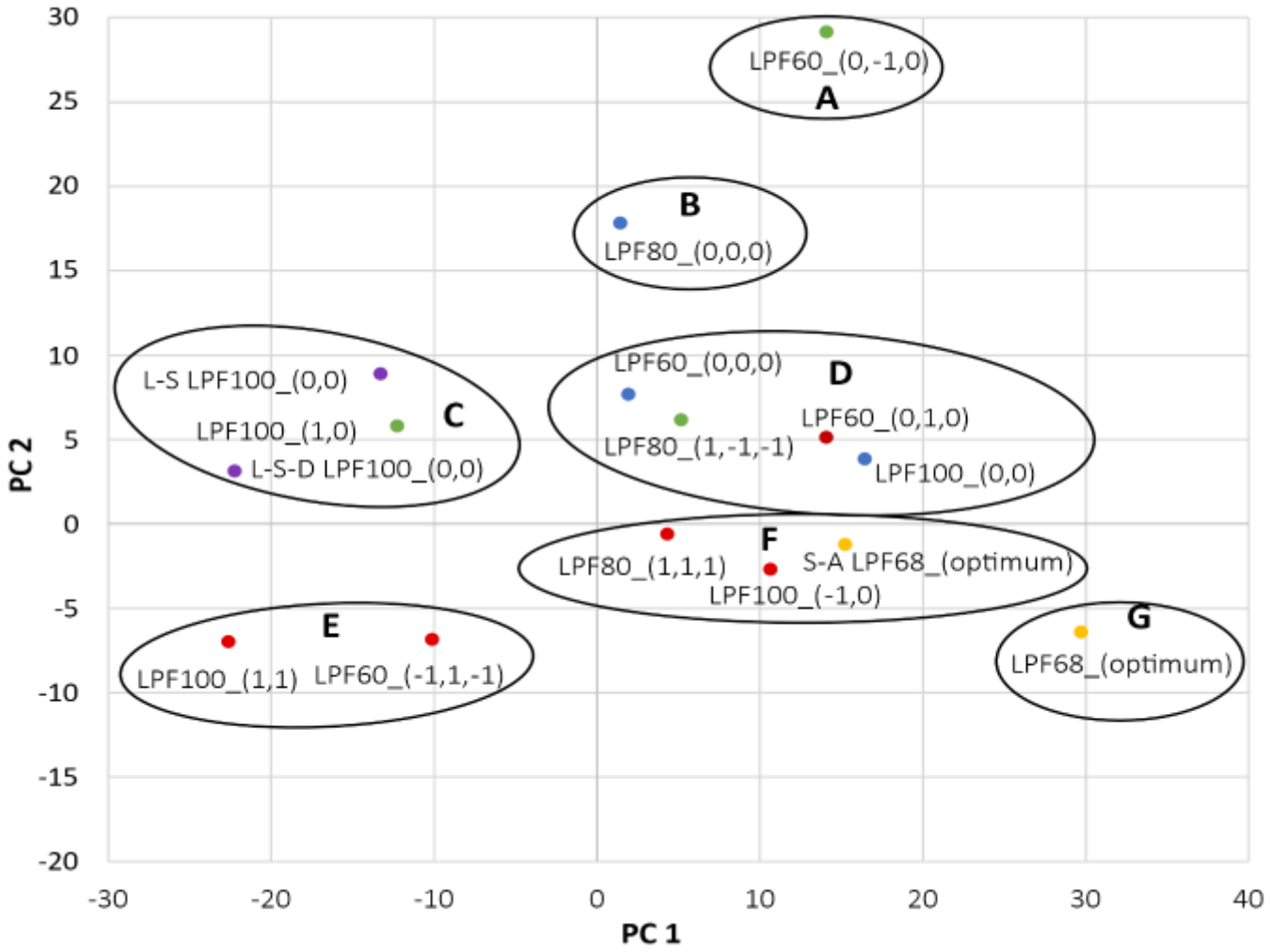

Figure 10

Scores plot of PC1 and PC2 from the mid-IR data of the different LPF resins

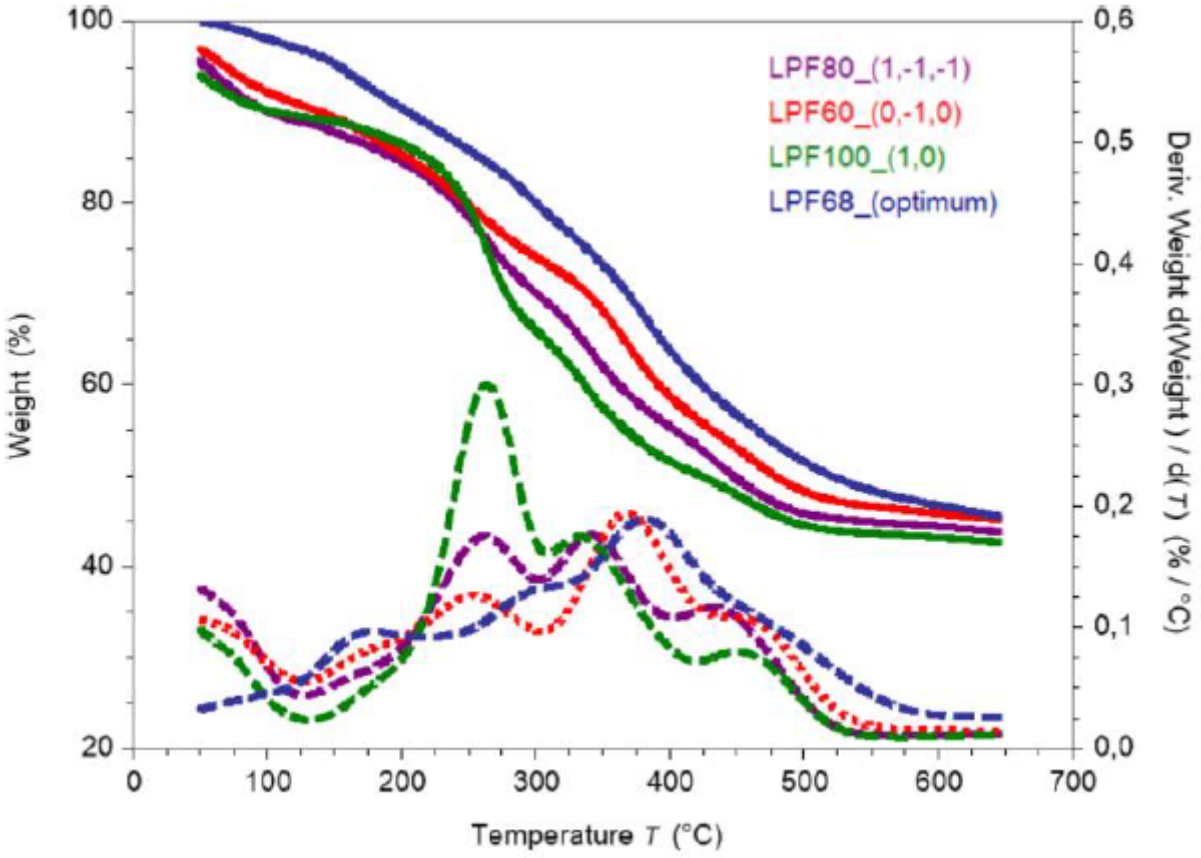

Figure 11

TGA and DTG graphs of the S-A-P LPF resins that produced the highest shear strength at different substitution levels

Supplementary Files

This is a list of supplementary files associated with this preprint. Click to download.

- Graphicalabstract.png